6.6 AN ENSEMBLE STUDY OF WET SEASON CONVECTION IN THE SOUTH WEST AMAZON: KINEMATICS AND IMPLICATIONS FOR DIABATIC HEATING

Robert Cifelli[1]*, Lawrence Carey[2], Walter A. Petersen[3], and Steven A. Rutledge[1]

[1] Colorado State University, Fort Collins, Colorado
[2] North Carolina State University, Raleigh, North Carolina
[3] University of Alabama-Huntsville, Huntsville, Alabama

1. INTRODUCTION

A number of previous studies have shown that the vertical distribution of diabatic heating, within tropical mesoscale precipitation systems (MCSs) can show considerable temporal and spatial variability (e.g., Houze 1989). Because general circulation models (GCM's) and numerical weather forecast models cannot explicitly resolve the diabatic effects resulting from MCSs, these processes must be parameterized. The Tropical Rainfall Measuring Mission (TRMM) was conceived in part to obtain a more accurate depiction of the four-dimensional distribution of diabatic (especially latent) heating across the global Tropics in order to improve modeling the tropical general circulation (Simpson et al. 1988).

The goal of this study is to examine the spectrum of convection sampled in southwest Amazonia during the Tropical Rainfall Measuring Mission Large Scale Biosphere-Atmosphere Experiment in Amazonia (TRMM-LBA) and quantify differences in kinematic and inferred diabatic heating structure across the ensemble of precipitation features that were sampled during the field program. Dual-Doppler radar syntheses are used to derive kinematic and diabatic heating characteristics of precipitation systems that were observed in January and February 1999 near Rondônia, Brazil during periods of low-level easterly flow (East Regime - ER) and low-level westerly flow (West Regime - WR).

Previous studies have shown that the ER and WR are forced by changes in the large scale patterns over South America and the position of the south Atlantic convergence zone (Rickenbach et al. 2002; Petersen et al. 2002). In the ER, convection typically occurs in high convective available potential energy (CAPE) and vertical shear environments and is more vertically developed and electrified compared to the WR (Cifelli et al. 2002; Halverson et al. 2002; Petersen et al. 2002).

2. METHODOLOGY

Data for this study were derived primarily from the S-POL and TOGA radars used during TRMM-LBA. Briefly, the NASA TOGA radar operates at C-band and collects reflectivity, radial velocity, and spectral width information. The NCAR S-POL radar operates at S-band and has dual-polarization capability. In addition to the parameters listed above for TOGA, S-POL also collected additional polarimetric variables including: differential reflectivity (Z_{DR}); linear depolarization ratio (LDR); total differential phase(Φ_{DP}); and zero lag correlation between co-polar horizontal and vertical polarized electromagnetic waves (ρ_{HV}).

For this study, an automated algorithm was utilized to unfold radial velocity measurements outside the radar Nyquist velocity range following a procedure described in Miller et al. (1986). Specifically, radial velocities were "locally" unfolded during the interpolation to caretesian space using the NCAR REORDER software package (Mohr et al., 1986). A "global" unfolding procedure was then employed using the NCAR CEDRIC (Custom Editing and Display of Reduced Information in Cartesian Space) software program (Mohr and Miller, 1983).

For a pair of TOGA and S-POL radar files to be combined in dual-Doppler synthesis, it was required that the radar volume be a plan position indicator (PPI) scan with the maximum elevation angle of at least 10º (corresponding to a height of 15 km at a range of 85 km) and that the start times of the two radar volumes be within 3 minutes of

* *Corresponding author address*: Robert Cifelli, Department of Atmospheric Science, Colorado State University, Fort Collins, CO 80523-1371; email: rob@atmos.colostate.edu

each other. Once all the candidate radar volumes were processed and the syntheses were complete, a program was utilized to compute 3-D histograms of radar reflectivity and vertical air motion for each synthesis volume. The histograms were used as a check to ensure that the synthesis results were reasonable. After the "bad" synthesis volumes were eliminated, a total of 2250 "good" synthesis volumes remained for subsequent analysis, representing some 260 hours of radar observations.

Precipitation features were classified into convective and weak convective-stratiform (WCSF) using a radar reflectivity horizontal texture algorithm (Cifelli et al. 2002).

3. RESULTS

Figures 1 and 2 show cumulative distributions of vertical air motion and radar reflectivity for the LBA ER and WR, respectively. The plots show that convection in the ER is characterized by more intense updrafts (Fig. 1) and larger radar reflectivities (Fig. 2) above the melting level, in agreement with ground and spaced-based lightning detection systems (Petersen et al. 2001).

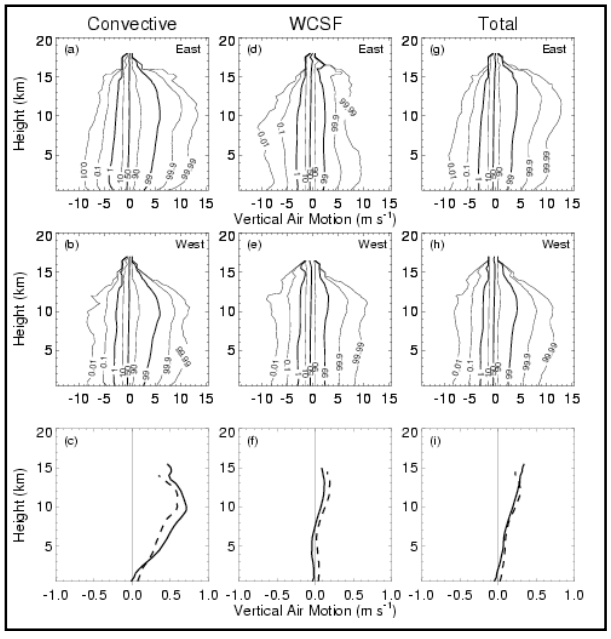

Figure 1. Cumulative frequency distributions of vertical air motion (m s^{-1}) for the ER (top row) and WR (middle row). The 1%, 50% and 99% contours are highlighted. The bottom row shows mean vertical air motion for the ER (solid) and WR (dashed). Panels from left to right in all rows represent convective, WCSF, and total (convective + WCSF).

The ER and WR kinematic and reflectivity differences are consistent with contrasts in composite thermal buoyancy between the regimes (Fig. 3): above the boundary layer, the environment in the ER is characterized by a greater magnitude and, more importantly, a larger gradient of virtual temperature excess for near surface rising parcels. The larger temperature excess would be expected to allow for stronger updrafts, more pronounced role of mixed phase microphysics, and more lightning in the ER.

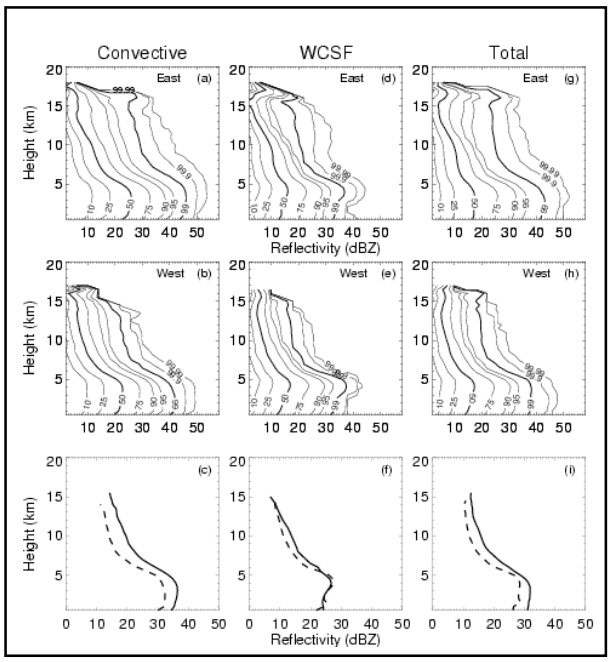

Figure 2. Same as Fig. 1 except for S-POL radar reflectivity (dBZ). The cumulative frequency distributions were constructed using a 4 dB bin size and 15 total bins.

The dual-Doppler data were then subdivided into four categories spanning the diurnal cycle. Both regimes showed a peak in intensity during the late afternoon hours, as evidenced by radar reflectivity (not shown) and kinematic characteristics (Fig. 4), consistent with previous studies of rainfall and lightning in the Rondônia (TRMM-LBA) region (Petersen et al. 2001; Rickenbach et al. 2002). After sunset however, convective intensity in the WR decreased much more abruptly compared to the ER. In the stratiform-weak convective region, the ER showed both reflectivity and kinematic characteristics of classic stratiform structure after sunset through the early morning hours, consistent with the lifecycle of MCSs. This latter feature was not observed in

the WR where convection was noted to largely dissipate without appreciable evolution from convective to stratiform morphology.

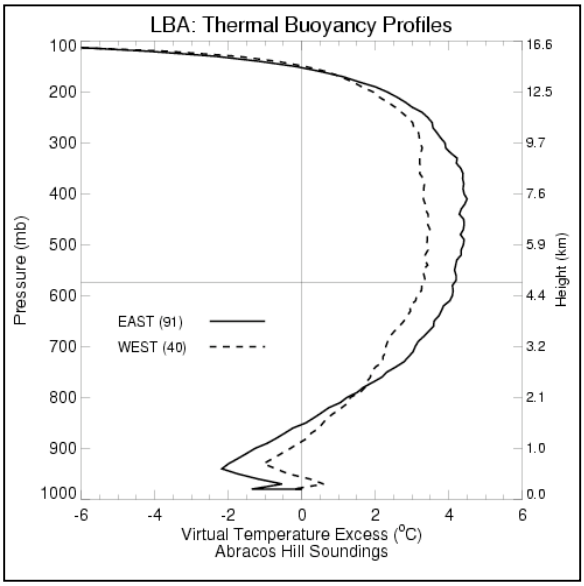

Figure 3. Pressure-height profiles of thermal buoyancy for the ER (solid) and WR (dashed). The 0°C level is indicated by the horizontal line. The number of soundings used in each profile composite is shown in the plot.

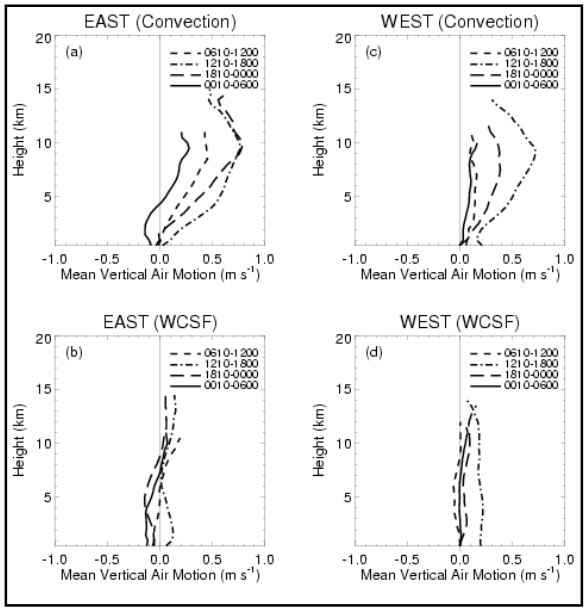

Figure 4. Mean vertical air motion profiles (m s^{-1}) for different periods of the diurnal cycle. Line patterns correspond to times (L) in each panel. East (West) profiles are shown in the left (right) columns with convection (WCSF) categories in the top (bottom) rows.

Apparent heating (Q_1) profiles were constructed for each regime assuming the vertical advection of dry static energy was the dominant forcing term. The resulting profiles show a peak centered near 8 km in the convective regions of both regimes, although the ER has a broader maximum compared to the WR (Fig. 5). The breadth of the ER diabatic heating peak is consistent with the more dominant role of ice processes in ER convection.

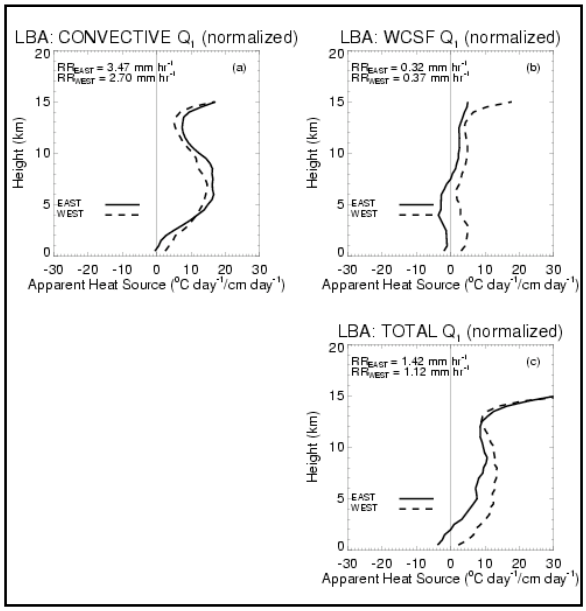

Figure 5. Height profiles of normalized Q_1 for the (a) convective region, (b) WCSF region, and (c) total (convective + WCSF region). In all panels, the East (West) profiles are indicated by the solid (dashed) lines. Average rain rates are indicated in each panel.

4. CONCLUSIONS

Consistent with thermodynamic characteristics of the environment, convection in the ER was shown to have larger magnitudes of vertical air motion, upper level divergence (not shown), and radar reflectivity compared to similar features in the WR. In the WCSF region, the major difference between the two regimes occurred in the lower troposphere. Moreover, the differences between ER and WR varied according to the phase of the diurnal cycle. In the ER, the intensity of convection increased markedly in the afternoon hours (1210-1800L) consistent with the cycle of solar insolation and equivalent potential temperature. After sunset, convective intensity generally decreased at low-levels but remained strong above the melting level, in agreement with

previous studies of lightning flash frequency and rainfall intensity. The overall pattern is consistent with the organization of precipitation into MCSs in the early evening hours. A similar cycle of convection occurred in the WR during the daytime hours; however, WR convection became significantly reduced after sunset.

Acknowledgements.

This work was supported by NASA TRMM grant NAG5-4754. The TRMM-LBA field program was carried out under the oversight of R. Kakar.

References

Cifelli, R., W.A. Petersen, L.D. Carey, and S.A. Rutledge, 2002: Radar Observations of the Kinematic, Microphysical, and Precipitation Characteristics of Two MCSs in TRMM-LBA. *J. Geophys. Res*, **107**, 10.1029/2000JD0000264.

Halverson, J.B., T. Rickenbach, B. Roy, H. Pierce, and E. Williams, 2002: Environmental characteristics of convective systems during TRMM-LBA. *Mon. Wea. Rev.*, **130**, 1493-1509.

Houze, R.A. Jr., 1989: Observed structure of mesoscale convective systems and implications for large-scale heating. *Quart. J. Roy. Meteor. Soc.*, **115**, 425-461.

Miller, J., C. G. Mohr, and A. J. Weinheimer, 1986: The simple rectification to Cartesian space of folded radial velocities from Doppler radar sampling. *J. Atmos. Oceanic Technol*, **3**, 162–174.

Mohr, C.G., and L.J. Miller, 1983: CEDRIC - a software package for cartesian space editing, synthesis, and display of radar fields under interactive control. Preprints*, 21st Conf. On Radar Meteorology*., Edmonton, Alta., Canada. Amer. Meteor. Soc., 559-574.

Mohr, C.G., L.J. Miller, R.L. Vaughan, and H.W. Frank, 1986: The merger of mesoscale datasets into a common cartesian format for efficient and systematic analyses. *J. Atmos. Oceanic Technol.*, **3**, 143-161.

Petersen, W.A., S.W. Nesbitt, R.J. Blakeslee, R. Cifelli, P. Hein, and S.A. Rutledge, 2001: TRMM observations of intraseasonal variability in convective regimes over the Amazon. *J. Climate*, **15**, 1278-1294.

Rickenbach, T.M., R.N. Ferreira, J. Halverson, and M.A.F. Silva Dias, 2002: Modulation of convection in the southwestern Amazon basin by extratropical stationary fronts. *J. Geophys. Res.*, **107**, 10.1029/2000JD000263.

Simpson, J., R.F. Adler and G.R. North, 1988: A proposed Tropical Rainfall Measuring Mission (TRMM) satellite. *Bull. Amer. Meteor. Soc.*, **69**, 278-295.